

Advanced adiabatic approximation for momentum distributions of ejected electrons in slow atomic collisions

T.P. Grozdanov^{1,a} and E.A. Solov'ev²

¹ Institute of Physics, P.O. Box 57, 11001 Belgrade, Yugoslavia

² The Macedonian Academy of Sciences and Arts, P.O. Box 428, 91000 Skopje, Macedonia

Received: 5 October 1998

Abstract. The problem of determination of momentum distributions of ejected electrons in slow atomic collisions is studied within the impact-parameter method by using a dynamic adiabatic basis which takes into account the correct boundary conditions. An expression is obtained which relates the momentum distribution of the ejected electrons with a coherent sum of the delocalized dynamic adiabatic eigenstates (elementary wavepackets). The form of the momentum distribution *exactly* coincides with the form of the total wavepacket in configuration space. General formulas are applied to a model problem of electron detachment in the process $A^- + A \rightarrow A + A + e$ in which the electron-atom interactions are described by the zero-range potentials. In the example considered, the momentum distribution of ejected electrons, in the center-of-mass frame, exhibits a maximum located in the scattering plane on the circle of radius $|\mathbf{k}| = (v/\rho)^{1/2}$ (in atomic units), where v is the relative collision velocity and ρ is the impact parameter.

PACS. 34.10.+x General theories and models of atomic and molecular collisions and interactions (including statistical theories, transition state, stochastic and trajectory models, etc.)

1 Introduction

In the theory of slow atomic collisions one can expect that the adiabatic electronic states of the quasimolecule formed during the collision play an essential role in the description of the collision dynamics. However, it is well known that these states are not compatible with physical boundary conditions. In the impact-parameter formulation of the theory (*i.e.* when the motion of the nuclei is described classically) it is necessary to append to molecular states the “electron translation factors” [1–4] in order to obtain a Galilean invariant theory.

An alternative approach is provided by the method of nonstationary scaling of length [5,6]. In this method the problem is reduced to the one in which the nuclei are at rest but additional dynamic interactions appear in the electronic Hamiltonian [7]. While the bound state adiabatic dynamics and the corresponding processes of excitation and charge exchange seem to be not strongly perturbed by these dynamic interactions [7–9], this may not be the case for the electron continuum states and the processes of ionization or detachment.

The theory of momentum distributions of the ejected electrons within the conventional adiabatic approach has been developed in reference [10]. This theory, however, not incorporating the momentum transfer effects, cannot be expected to correctly describe the region where the veloci-

ties of the ejected electrons are smaller than or of the order of magnitude of the relative collision velocity. The above-mentioned method of nonstationary scaling of length has been originally introduced in order to eliminate this defect and has been successfully applied to some exactly solvable models [5,11]. More recently, based on this method, an *ab initio* treatment of the spectra of ejected electrons, involving expansions in two-center Sturmian bases has been developed [12,13]. Our goal in the present paper is to introduce an approximate, adiabatic theory, valid for slow collisions, which properly incorporates momentum transfer effects and still provides a physically transparent picture of adiabatic mechanisms of the electron promotions into the continuum.

The plan of the article is as follows. In Section 2 we give the general formulation of the theory and derive basic formulas for the momentum distributions of ejected electrons. Some specific features of symmetric (homonuclear) collisional systems are also discussed. In Section 3 the theory is applied to a three-dimensional model describing the detachment process: $A + A^- \rightarrow A + A + e$ in which the electron-atom interactions are simulated by the zero-range potentials. Finally, Section 4 contains concluding remarks.

2 General theory

Let us consider a collisional system consisting of an electron and two centers of central forces traveling along the

^a e-mail: egrozdan@ubbg.etf.bg.ac.yu

given classical trajectories. We label the centers T (target) and P (projectile) and assume the rectilinear trajectories, although generalizations to curved trajectories are straightforward. The electron wave function is a solution of the time-dependent Schrödinger equation (we use atomic units throughout the work):

$$\left[-\frac{1}{2}\nabla_{\mathbf{r}}^2 + V_T(|\mathbf{r} + \alpha\mathbf{R}(t)|) + V_P(|\mathbf{r} - \beta\mathbf{R}(t)|) \right] \times \psi(\mathbf{r}, t) = i\frac{\partial}{\partial t}\psi(\mathbf{r}, t), \quad (2.1)$$

where $\mathbf{R}(t) = \mathbf{R}_P(t) - \mathbf{R}_T(t) = (vt, \rho, 0)$ is the internuclear vector, v is the relative collision velocity, ρ is the impact parameter and parameters α and β ($\alpha + \beta = 1$) define the position of the origin of the chosen reference frame which is located on the internuclear axis ($\mathbf{R}_T(t) = -\alpha\mathbf{R}(t)$, $\mathbf{R}_P(t) = \beta\mathbf{R}(t)$). If initially ($t \rightarrow -\infty$) the electron is bound at the target in an atomic state defined by the wave function $\phi_i(\mathbf{r}_T)$ and energy E_i , then we are looking for the solution of (2.1) satisfying the following boundary condition:

$$\lim_{t \rightarrow -\infty} \psi(\mathbf{r}, t) \sim \phi_i(\mathbf{r}_T) \times \exp \left[i \left(\mathbf{v}_T \cdot \mathbf{r}_T + \frac{1}{2}v_T^2 t - E_i t \right) \right], \quad (2.2)$$

where $\mathbf{r}_T = \mathbf{r} - \mathbf{R}_T$, $\mathbf{v}_T = -\alpha\mathbf{v}$ is the velocity of the target and the Galilean translational factor takes into account the motion of the target in the chosen reference frame.

We introduce the nonstationary scaling of length by dividing electron coordinates (x, y, z) by the internuclear separation $R(t)$ and simultaneously making the transformation to the rotating reference frame $\{\hat{q}_1, \hat{q}_2, \hat{q}_3\}$ with the unit vector of the q_1 -axis directed along the internuclear axis ($\hat{q}_1 = \hat{R}(t)$). The scaled coordinates are related to the original ones by

$$q_1 = \frac{1}{R(t)}[x \cos \varphi(t) + y \sin \varphi(t)], \quad (2.3)$$

$$q_2 = \frac{1}{R(t)}[-x \sin \varphi(t) + y \cos \varphi(t)], \quad (2.4)$$

$$q_3 = \frac{z}{R(t)}, \quad (2.5)$$

where $\varphi(t) = \arctan(\rho/vt)$ is the polar angle of the $\mathbf{R}(t)$ in the scattering plane. The electron wave function is represented in the form

$$\psi(\mathbf{r}, t) = R^{-\frac{3}{2}}(t) \exp \left[i \frac{r^2}{2R(t)} \frac{dR(t)}{dt} \right] f(\mathbf{q}, \tau) \quad (2.6)$$

and a new time-like variable is introduced:

$$\tau(t) = \int_0^t \frac{dt'}{R^2(t')} = \omega^{-1} \arctan \left(\frac{vt}{\rho} \right), \quad (2.7)$$

with $\omega = \rho v$. The factor $R^{-\frac{3}{2}}(t)$ in (2.6) ensures the normalization and the exponent is the generalized translational factor. The variation of the time in the interval

$-\infty < t < +\infty$ corresponds to the variation of the parameter τ in the interval $-\pi/(2\omega) < \tau < \pi/(2\omega)$. Substituting (2.3-2.7) into (2.1) we obtain the modified Schrödinger equation

$$H(\tau)f(\mathbf{q}, \tau) = i\frac{\partial f(\mathbf{q}, \tau)}{\partial \tau}, \quad (2.8)$$

with

$$H(\tau) = -\frac{1}{2}\nabla_{\mathbf{q}}^2 + R^2(\tau)[V_T(R(\tau)|\mathbf{q} + \alpha\hat{q}_1|) + V_P(R(\tau)|\mathbf{q} - \beta\hat{q}_1|)] + \omega L_3 + \frac{1}{2}\omega^2 q^2, \quad (2.9)$$

where $R(\tau) = \rho/\cos \omega\tau$ and

$$L_3 = -i \left(q_1 \frac{\partial}{\partial q_2} - q_2 \frac{\partial}{\partial q_1} \right) \quad (2.10)$$

is the operator of the projection of the electron angular momentum perpendicular to the scattering plane. In the new (\mathbf{q}, τ) "representation" the potential centers are at "rest", but as seen from (2.9) both the range and the strength of the potentials are τ -dependent. The Hamiltonian $H(\tau)$ is an even function of τ and the parity $\Pi(q_3 \rightarrow -q_3)$ is an exact symmetry.

The generalized translational factor has the important property

$$\lim_{Rr_X^{-1} \rightarrow \infty} \exp \left[i \frac{r^2}{2R(t)} \frac{dR(t)}{dt} \right] \sim \exp \left[i \left(\frac{1}{R(t)} \frac{dR(t)}{dt} \mathbf{R}_X(t) \cdot \mathbf{r}_X + \frac{R_X^2(t)}{2R(t)} \frac{dR(t)}{dt} \right) \right], \quad (2.11)$$

where $X = T, P$. This is possible either when $r_X \rightarrow 0$ and R is finite or when r_X is finite and $R \rightarrow \infty$. In the latter case, which corresponds to $t \rightarrow \pm\infty$, we further have

$$\lim_{t \rightarrow \pm\infty} \exp \left[i \left(\frac{1}{R(t)} \frac{dR(t)}{dt} \mathbf{R}_X(t) \cdot \mathbf{r}_X + \frac{R_X^2(t)}{2R(t)} \frac{dR(t)}{dt} \right) \right] \sim \exp \left[i \left(\mathbf{v}_X \cdot \mathbf{r}_X + \frac{1}{2}v_X^2 t \right) \right], \quad (2.12)$$

giving the complete Galilean translation factor. As a consequence, the boundary condition associated with equation (2.8) and corresponding to (2.2) reads

$$\lim_{\tau \rightarrow \tau_i + 0} f(\mathbf{q}, \tau) \sim R^{\frac{3}{2}}(\tau) e^{i\pi L_{3T}} \phi_i(\mathbf{q}_T R(\tau)) e^{-iE_i \int^\tau R^2(\tau') d\tau'}, \quad (2.13)$$

with $\mathbf{q}_T = \mathbf{q} + \alpha\hat{q}_1$. The rotational operator is introduced above due to the mutual orientation of the two reference frames at $t \rightarrow -\infty$ as defined by (2.3-2.5). Note that that it does not affect, for example, spherically symmetric initial atomic states.

In slow collisions, in order to solve (2.8), it is natural to expand $f(\mathbf{q}, \tau)$ in terms of the adiabatic (instantaneous) eigenfunctions of $H(\tau)$. Note that in general the spectrum

of $H(\tau)$ is discrete (the exception is the case of head-on collisions, $\rho = 0, \omega = 0$). It is important to distinguish between the three subsets of these dynamic adiabatic eigenstates, which we label by the index $X = T, P, C$:

$$f(\mathbf{q}, \tau) = \sum_{X=T,P,C} \sum_{\alpha_X} a_{\alpha_X}(\tau) \chi_{\alpha_X}(\mathbf{q}, \tau) e^{-i \int^{\tau} \varepsilon_{\alpha_X}(\tau') d\tau'}, \quad (2.14)$$

where

$$H(\tau) \chi_{\alpha_X}(\mathbf{q}, \tau) = \varepsilon_{\alpha_X}(\tau) \chi_{\alpha_X}(\mathbf{q}, \tau). \quad (2.15)$$

The three subsets differ in their behavior in the asymptotic region defined by $R \rightarrow +\infty$ (i.e. $t \rightarrow \pm\infty, \tau \rightarrow \tau_{i,f}$). The first two subsets ($X = T, P$) represent the states asymptotically localized in the vicinity of the potential centers ($q_X \rightarrow 0$) and, in this limit, are given by [9]

$$\lim_{\tau \rightarrow \tau_{i,f}} \chi_{\alpha_X}(\mathbf{q}, \tau) \sim R^{\frac{3}{2}}(\tau) \phi_{\alpha_X}(\mathbf{q}_X R(\tau)), \quad (2.16)$$

$$\lim_{\tau \rightarrow \tau_{i,f}} \varepsilon_{\alpha_X}(\tau) \sim E_{\alpha_X} R^2(\tau), \quad (2.17)$$

where $\phi_{\alpha_{T,P}}(\mathbf{r}_{T,P})$ and $E_{\alpha_{T,P}}$ are separated-atom limits of adiabatic quasimolecular states and energies corresponding to bound states in isolated potentials $V_{T,P}(r_{T,P})$. When transformed back to (\mathbf{r}, t) variables by means of relations (2.6), (2.11) and (2.12), these states correspond asymptotically to traveling atomic states. Note also that $\varepsilon_{\alpha_{T,P}}(\tau) \rightarrow -\infty$ when $R \rightarrow +\infty$.

The third subset ($X = C$) represents states with $\varepsilon_{\alpha_C} > 0$, which are not localized in any particular region of the configuration space and whose asymptotic behavior for $q \rightarrow +\infty$ is mainly determined by the oscillator potential in (2.9). The particular form of these states and their behavior when $R \rightarrow +\infty$ depend on the specific properties of the interaction potentials V_T and V_P . An example will be given in the next section. When transformed back to (\mathbf{r}, t) variables by means of relation (2.6), these states represent spreading wavepackets in the continuum and are therefore of basic importance for the description of ionization or detachment processes.

The unknown expansion amplitudes $a_{\alpha_X}(\tau)$ in (2.14) can be determined from the usual set of coupled equations:

$$\begin{aligned} \frac{da_{\alpha_X}(\tau)}{d\tau} = & - \sum_{X'=T,P,C} \sum_{\alpha'_{X'} \neq \alpha_X} \left\langle \chi_{\alpha_X} \left| \frac{\partial}{\partial \tau} \right| \chi_{\alpha'_{X'}} \right\rangle \\ & \times a_{\alpha'_{X'}}(\tau) e^{-i \int^{\tau} [\varepsilon_{\alpha'_{X'}}(\tau') - \varepsilon_{\alpha_X}(\tau')] d\tau'}. \end{aligned} \quad (2.18)$$

The initial conditions associated with (2.18) should be in accord with (2.13). If the initial atomic state belongs to a degenerate subspace then in general we have several of $a_{\alpha_T}(\tau_i) \neq 0$. The simplest is the case when the initial state is non-degenerate spherically symmetric state, so that it coincides with one of the separated-atom limits of the quasimolecular states ($i \equiv \alpha_T^0$):

$$a_{\alpha_X}(\tau_i) = \delta_{\alpha_X, \alpha_T^0}. \quad (2.19)$$

The information on various inelastic processes can be extracted from the asymptotic values of the amplitudes $a_{\alpha_X}(\tau_f)$. In order to do this, we first note that as a consequence of (2.14) the wave function in (\mathbf{r}, t) variables can be written as a sum of three orthogonal terms:

$$\psi(\mathbf{r}, t) = \sum_{X=T,P,C} \psi_X(\mathbf{r}, t). \quad (2.20)$$

For $X = T, P$ and $t \rightarrow +\infty$ we have from (2.11), (2.12) and (2.16):

$$\begin{aligned} \lim_{t \rightarrow +\infty} \psi_X(\mathbf{r}, t) \sim & e^{i\mathbf{v}_X \cdot \mathbf{r}_X + \frac{1}{2} v_X^2 t} \\ & \times \sum_{\alpha_X} a_{\alpha_X}(\tau_f) \phi_{\alpha_X}(\mathbf{r}_X) e^{-i \int^t \varepsilon_{\alpha_X}(t') R^{-2}(t') dt'}. \end{aligned} \quad (2.21)$$

These wave functions describe superpositions of electron bound states traveling with the potential centers. The probabilities for the excitation and charge exchange are given by

$$P_{\text{exc}}(\rho, v) = \sum_{\alpha_T \neq \alpha_T^0} |a_{\alpha_T}(\tau_f)|^2, \quad (2.22)$$

$$P_{\text{cex}}(\rho, v) = \sum_{\alpha_P} |a_{\alpha_P}(\tau_f)|^2. \quad (2.23)$$

The corresponding cross-sections can be obtained by integrating over the impact parameters.

The electrons ejected into the continuum are described by the wave function

$$\begin{aligned} \psi_C(\mathbf{r}, t) = & R^{-\frac{3}{2}}(t) e^{i \frac{r^2}{2R(t)} \frac{dR(t)}{dt}} \\ & \times \sum_{\alpha_C} a_{\alpha_C}(\tau) \chi_{\alpha_C}(\mathbf{q}, \tau) e^{-i \int^{\tau} \varepsilon_{\alpha_C}(\tau') d\tau'}. \end{aligned} \quad (2.24)$$

The quantity of interest is the momentum distribution of the ejected electrons:

$$\begin{aligned} W(\mathbf{k}) = & \left| \lim_{t \rightarrow +\infty} (2\pi)^{-\frac{3}{2}} \int e^{-i\mathbf{k} \cdot \mathbf{r} + i \frac{1}{2} k^2 t} \psi_C(\mathbf{r}, t) d^3 \mathbf{r} \right|^2. \end{aligned} \quad (2.25)$$

The integral can be evaluated by the saddle-point method (see Appendix A), giving our main result:

$$\begin{aligned} W(\mathbf{k}) = & v^{-3} \left| \sum_{\alpha_C} a_{\alpha_C}(\tau_f) \chi_{\alpha_C} \left(\frac{\mathbf{k}}{v}, \tau_f \right) e^{-i \int^{\tau_f} \varepsilon_{\alpha_C}(\tau) d\tau} \right|^2. \end{aligned} \quad (2.26)$$

The above expression indicates that the form of the momentum distribution of the ejected electrons is determined by the coherent superposition of those dynamic adiabatic eigenstates $\chi_{\alpha_C}(\mathbf{k}/v, \tau_f)$ which are populated during the collision. Comparing sums in (2.24) and (2.26), one can see that both expressions are the same function referred

to different (configuration and momentum) spaces. This is due to an interesting property of the wave function of ejected electron. Namely its invariance (up to a universal phase factor — the generalized translational factor) with respect to Fourier transform which connects the configuration and momentum representations. The total probability for the break-up process (ionization or detachment) is

$$P_{\text{ion}}(\rho, v) = \int W(\mathbf{k}) d^3\mathbf{k} = \sum_{\alpha_C} |a_{\alpha_C}(\tau_f)|^2, \quad (2.27)$$

which directly follows from (2.26) due to the orthonormalization of the adiabatic eigenfunctions.

We conclude this section by discussing some specific modifications which are necessary in the case of symmetric (homonuclear) collision systems. In our formulation these systems are defined by the condition: $V_T(r) = V_P(r)$. The common origin of both rotating and non-rotating reference frames is taken at the midpoint of the internuclear axis ($\alpha = \beta = 1/2$). The dynamic adiabatic eigenstates can now be divided into two groups of symmetric or even-parity (g) and antisymmetric or odd-parity (u) states with respect to the transformation: $\mathbf{q} \rightarrow -\mathbf{q}$. In addition, the index X used above to distinguish between the localized and delocalized states takes now only two values: $X = B, C$. This is because the asymptotically bound adiabatic eigenstates are in this case localized simultaneously around both centers. Instead of the expansion (2.14) we now have

$$f(\mathbf{q}, \tau) = \sum_{s=g,u} \sum_{X=B,C} \sum_{\alpha_X} a_{\alpha_X}^s(\tau) \chi_{\alpha_X}^s(\mathbf{q}, \tau) e^{-i \int_{\tau_i}^{\tau} \varepsilon_{\alpha_X}^s(\tau') d\tau'}. \quad (2.28)$$

The first group of states ($X = B$) represents now asymptotically the symmetric and antisymmetric combinations of atomic states:

$$\lim_{\tau \rightarrow \tau_{i,f}} \chi_{\alpha_B}^{g,u}(\mathbf{q}, \tau) \sim R^{\frac{3}{2}}(\tau) 2^{-\frac{1}{2}} [\phi_{\alpha_B}(\mathbf{q}_T R(\tau)) \pm \phi_{\alpha_B}(-\mathbf{q}_P R(\tau))], \quad (2.29)$$

$$\lim_{\tau \rightarrow \tau_{i,f}} \varepsilon_{\alpha_B}^{g,u}(\tau) \sim E_{\alpha_B} R^2(\tau). \quad (2.30)$$

The coupled equations for g and u amplitudes $a_{\alpha_X}^{g,u}(\tau)$ decouple and can be solved independently. The initial conditions are again particularly simple in the case of a spherically symmetric non-degenerate initial atomic state $\phi_{\alpha_B}^0(r_T)$ on the target T :

$$a_{\alpha_X}^{g,u}(\tau_i) = 2^{-\frac{1}{2}} \delta_{\alpha_X, \alpha_B^0}. \quad (2.31)$$

The probabilities for the excitation and charge exchange are now given by

$$P_{\text{exc}}(\rho, v) = \frac{1}{2} \sum_{\alpha_B \neq \alpha_B^0} \left| a_{\alpha_B}^g(\tau_f) e^{-i \int_{\tau_i}^{\tau_f} \varepsilon_{\alpha_B}^g(\tau') d\tau'} + a_{\alpha_B}^u(\tau_f) e^{-i \int_{\tau_i}^{\tau_f} \varepsilon_{\alpha_B}^u(\tau') d\tau'} \right|^2, \quad (2.32)$$

$$P_{\text{cex}}(\rho, v) = \frac{1}{2} \sum_{\alpha_B} \left| a_{\alpha_B}^g(\tau_f) e^{-i \int_{\tau_i}^{\tau_f} \varepsilon_{\alpha_B}^g(\tau') d\tau'} - a_{\alpha_B}^u(\tau_f) e^{-i \int_{\tau_i}^{\tau_f} \varepsilon_{\alpha_B}^u(\tau') d\tau'} \right|^2. \quad (2.33)$$

The probability distribution of the ejected electrons is

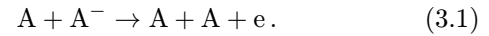
$$W(\mathbf{k}) = v^{-3} \left| \sum_{s=g,u} \sum_{\alpha_C} a_{\alpha_C}^s(\tau_f) \chi_{\alpha_C}^s \left(\frac{\mathbf{k}}{v}, \tau_f \right) \times e^{-i \int_{\tau_i}^{\tau_f} \varepsilon_{\alpha_C}^s(\tau) d\tau} \right|^2, \quad (2.34)$$

and the total ionization or detachment probability is

$$P_{\text{ion}}(\rho, v) = \sum_{\alpha_C} (|a_{\alpha_C}^g(\tau_f)|^2 + |a_{\alpha_C}^u(\tau_f)|^2). \quad (2.35)$$

3 Model problem with zero-range potentials

The general theory presented in the previous section is applied here to a model problem describing the detachment of an electron from a negative ion colliding with its own atom:



The interaction of the active electron with each of the atoms is described by the zero-range potential [14]:

$$V_X = \frac{2\pi}{\gamma} \delta(\mathbf{r}_X) \frac{\partial}{\partial r_X} r_X, \quad (3.2)$$

where $X = T, P$ and $\mathbf{r}_{T,P} = \mathbf{r} \pm \frac{1}{2}\mathbf{R}(t)$. Parameter $\gamma > 0$ defines the energy $E_B = -\gamma^2/2$ of a single bound state supported by an isolated zero-range potential. The corresponding eigenfunction is

$$\phi_B(r_X) = \left(\frac{\gamma}{2\pi} \right)^{\frac{1}{2}} \frac{e^{-\gamma r_X}}{r_X}. \quad (3.3)$$

Alternatively, instead of dealing with the operators (3.2) the existence of the zero-range potentials is equivalent to imposing additional boundary conditions onto the electron wave function [14]:

$$\lim_{r_X \rightarrow 0} \psi(\mathbf{r}, t) \sim c(t) \left(\frac{1}{r_X} - \gamma + i\mathbf{v}_X \cdot \hat{r}_X \right). \quad (3.4)$$

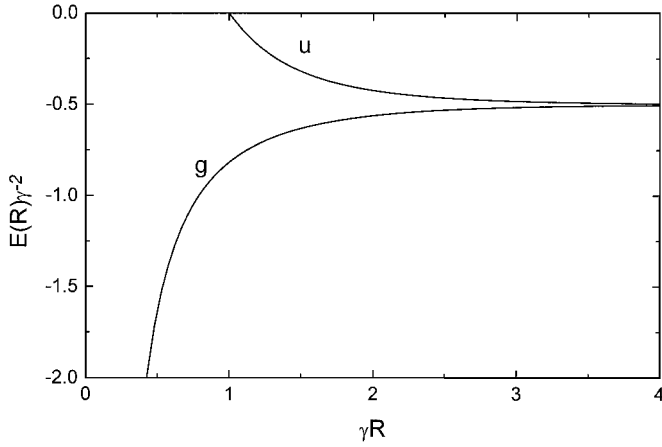


Fig. 1. Adiabatic eigenvalues (potential energy curves) of symmetric (g) and antisymmetric (u) states of an electron in the field of two identical zero-range potentials as functions of internuclear distance R .

The usual Born-Oppenheimer adiabatic potential energy curves of this collisional system can be found as solutions of the transcendental equation [14]:

$$(-2E)^{\frac{1}{2}} \mp \frac{1}{R} \exp \left[-(-2E)^{\frac{1}{2}} R \right] = \gamma. \quad (3.5)$$

The dependence of the potential energy curves corresponding to symmetric (g) and antisymmetric (u) states on the internuclear separation R is shown in Figure 1. The initial electron wave function in the process (3.1) is a symmetric combination of g - and u - asymptotic adiabatic states, and these components evolve independently in time. From Figure 1 it can be seen that the crossing of the continuum border of the u -curve at $R = 1/\gamma$ is responsible for the promotion of the electron into continuum leading to the detachment process. The g -curve stays all the time far from the continuum and this component is not expected to contribute to the detachment. Note, however, that the model is pathological in the united atom limit $R \rightarrow 0$, because there is a non-physical divergence of the g -curve which behaves like $\sim -\text{const}/R^2$.

Although the above adiabatic picture is physically transparent, as mentioned in the Introduction, the Born-Oppenheimer states do not take into account the motion of the centers, and one has to resort to dynamic adiabatic states, that is to the solutions of (2.15). For this system, dynamic adiabatic eigenfunctions can be found in the closed form (see Appendix B):

$$\chi^{g,u}(\mathbf{q}, \tau) = N \left[e^{\frac{i}{2}\omega q_2} \frac{1}{q_T} U \left(-\frac{\varepsilon(\tau)}{\omega}, (2\omega)^{\frac{1}{2}} q_T \right) \pm e^{-\frac{i}{2}\omega q_2} \frac{1}{q_P} U \left(-\frac{\varepsilon(\tau)}{\omega}, (2\omega)^{\frac{1}{2}} q_P \right) \right], \quad (3.6)$$

where $q_{T,P} = |\mathbf{q} \pm \frac{1}{2}\hat{q}_1|$, N is a normalization constant and $U(a, x) \equiv D_{-a-\frac{1}{2}}(x)$ is the parabolic-cylinder function [15]. The dynamic adiabatic eigenvalues $\varepsilon(\tau)$ are all

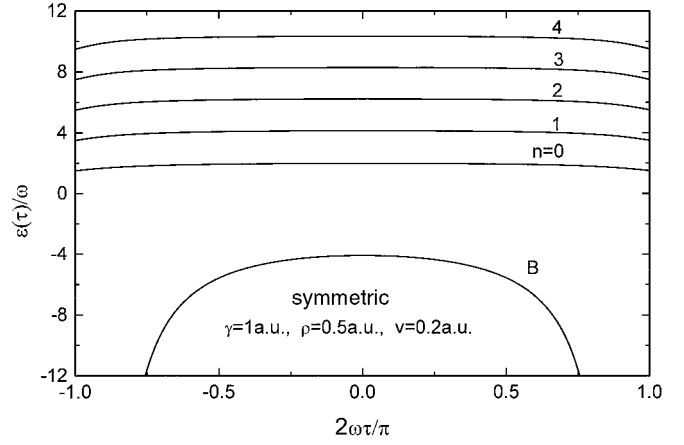


Fig. 2. Dynamic adiabatic eigenvalues of symmetric states as functions of time-like parameter τ .

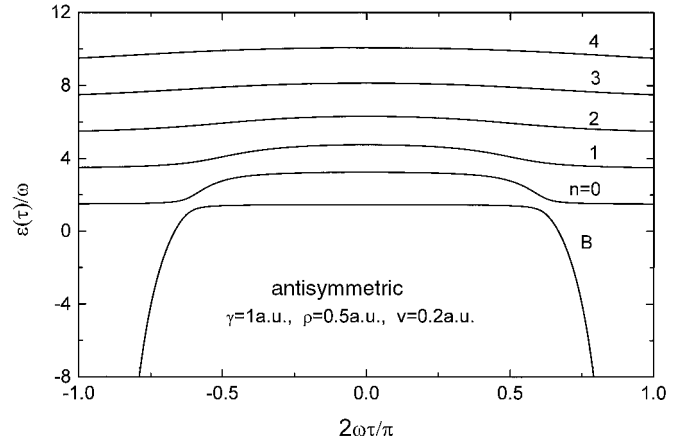


Fig. 3. Same as Figure 2 but for antisymmetric states.

possible solutions of the equation

$$(2\omega)^{\frac{1}{2}} U' \left(-\frac{\varepsilon}{\omega}, 0 \right) \pm U \left(-\frac{\varepsilon}{\omega}, (2\omega)^{\frac{1}{2}} \right) = -\gamma R(\tau) U \left(-\frac{\varepsilon}{\omega}, 0 \right), \quad (3.7)$$

where prime indicates the derivative with respect to the second argument and $R(\tau) = \rho / \cos \omega \tau$. In all numerical calculations we have used rapidly convergent power series expansions of $U(a, x)$ [15].

Two examples of dynamic adiabatic eigenvalues as functions of the parameter τ are shown in Figure 2 (symmetric states) and Figure 3 (antisymmetric states) for the set of parameters: $\gamma = 1$ a.u., $\rho = 0.5$ a.u. and $v = 0.2$ a.u. Before we proceed further, we note that, as has already been indicated in figure 1, our problem possesses an exact scaling property. This means that once we have certain results for $\gamma = 1$ a.u., the results for an arbitrary γ can be obtained by scaling all lengths by γ^{-1} , all momenta by γ , energies by γ^{-2} and so on.

As can be seen from Figures 2 and 3 in each of these cases there is only one asymptotically bound state, which we, following the notation of the preceding section ($X = B$) simply call B -type state and label as $\alpha_B = B$. These

states for $\tau \rightarrow \tau_{i,f}$ (that is $R(\tau) \rightarrow +\infty$) are characterized by $\varepsilon_B^{g,u}(\tau) \rightarrow -\infty$. Therefore, in this limit, in both (3.6) and (3.7) we can use the asymptotic formula [15]:

$$U(a, x) \sim U(a, 0) \exp \left[-a^{\frac{1}{2}} x + O(a^{-\frac{1}{2}}) \right], \quad (3.8)$$

valid for $a \gg x^2$, as well as the exact expressions [15]:

$$\begin{aligned} U(a, 0) &= \frac{(\pi)^{\frac{1}{2}}}{2^{\frac{a}{2} + \frac{1}{4}} \Gamma\left(\frac{3}{4} + \frac{a}{2}\right)}, \\ U'(a, 0) &= -\frac{(\pi)^{\frac{1}{2}}}{2^{\frac{a}{2} - \frac{1}{4}} \Gamma\left(\frac{1}{4} + \frac{a}{2}\right)}, \end{aligned} \quad (3.9)$$

in order to obtain

$$\lim_{\tau \rightarrow \tau_{i,f}} \chi_B^{g,u}(\mathbf{q}, \tau) \sim N' \left[\frac{e^{-(2\varepsilon)^{\frac{1}{2}} q_T}}{q_T} \pm \frac{e^{-(2\varepsilon)^{\frac{1}{2}} q_P}}{q_P} \right], \quad (3.10)$$

$$(-2\varepsilon)^{\frac{1}{2}} \mp e^{-(2\varepsilon)^{\frac{1}{2}}} = \gamma R(\tau). \quad (3.11)$$

Note that if we introduce $E = \varepsilon R^{-2}$, then (3.11) transforms exactly into (3.5), giving the relationship between the usual and dynamic adiabatic eigenvalues in the asymptotic region. If we neglect the exponentially small splitting between the g - and u -eigenvalues, then from (3.11) we find

$$\lim_{\tau \rightarrow \tau_{i,f}} \varepsilon_B^{g,u}(\tau) \sim -\frac{\gamma^2}{2} R^2(\tau), \quad (3.12)$$

which is in accord with (2.30). Substituting (3.12) into (3.10) and taking into account (3.3) we see that (2.29) is also fulfilled.

We now turn to the remaining set ($X = C$, C -type states) of the dynamic eigenvalues shown in Figures 2 and 3 and labeled by $\alpha_C \equiv n = 0, 1, 2, \dots$. All these eigenvalues have the property

$$\varepsilon_n^{g,u}(\tau_{i,f}) = \omega \left(2n + \frac{3}{2} \right). \quad (3.13)$$

This result directly follows from (3.7) and (3.9), because the poles of the function $R(\varepsilon)$ coincide with the poles of the gamma-function $\Gamma\left(\frac{3}{4} - \frac{\varepsilon}{2\omega}\right)$, that is with (3.13). Substituting (3.13) in (3.6) we find the asymptotic expression of the C -type dynamic adiabatic eigenstates:

$$\begin{aligned} \chi_n^{g,u}(\mathbf{q}, \tau_{i,f}) &= N_n \left[e^{-\frac{\omega}{2}(q_T^2 - iq_2)} L_n^{\frac{1}{2}}(\omega q_T^2) \pm \right. \\ &\quad \left. \pm e^{-\frac{\omega}{2}(q_P^2 + iq_2)} L_n^{\frac{1}{2}}(\omega q_P^2) \right], \end{aligned} \quad (3.14)$$

where $L_n^\alpha(x)$ are generalized Laguerre polynomials [15].

In the case of the symmetric states, as can be seen from Figure 2, the B -type state is well separated from C -type states, the latter being only slightly perturbed from their asymptotic values (3.13). Therefore, the transitions from a symmetric component of an initial bound state to C -type states, which lead to detachment, can be neglected. This

is in accord with the above given discussion in connection with Figure 1.

On the contrary, as seen from Figure 3, antisymmetric B -type state is strongly coupled to a few C -type states, exhibiting the characteristic avoided crossings of eigenvalues. This is also in accord with the discussion related to Figure 1, where it was predicted that it is the antisymmetric component of the wave function which is responsible for the detachment process.

In order to find transition amplitudes, one has to solve the corresponding system of coupled equations with initial conditions (2.31) with $\alpha_T^0 \equiv B$. Alternatively, we shall adopt an approximate adiabatic method based on the existence of ‘‘hidden crossings’’ [7] which is asymptotically exact in the limit $v \rightarrow 0$. This method relies on the fact that the adiabatic eigenvalues, such as those of antisymmetric states shown in Figure 3, represent various branches of a single multivalued analytic function $\varepsilon^u(\tau)$ which is in our case implicitly defined by equation (3.7). Various branches can be analytically continued from the real τ -axis into complex τ -plane. The positions of branch points (points of exact degeneracy of the pairs of complex eigenvalues) are essential for determination of the transition amplitudes between the adiabatic eigenstates [7, 16].

In our case we first determine, using equation (3.7), the branch points of the multivalued analytic function $\varepsilon^u(R)$ in the complex R -plane, and then we use the analytic continuation of the relation (2.7)

$$\tau = \frac{i}{2\omega} \ln \frac{i + \left[\left(\frac{R}{\rho} \right)^2 - 1 \right]^{\frac{1}{2}}}{i - \left[\left(\frac{R}{\rho} \right)^2 - 1 \right]^{\frac{1}{2}}}, \quad (3.15)$$

to calculate the branch points in the complex τ -plane. In actual calculations we use the fact that in the vicinity of the branch point $R = R_c$ we have $\varepsilon^u(R) = \varepsilon_c^u + C(R - R_c)^{\frac{1}{2}}$. Therefore, we can find branch points by searching for the points, where $dR/d\varepsilon^u = 0$ and the function $R(\varepsilon^u)$ is explicitly given by (3.7). For parabolic-cylinder functions $U(a, x)$ and its derivatives, analytic continuations of the power-series expansions [15] have been used.

Figure 4 shows the branch points in the first quadrant of the complex τ -plane for the three cases defined by the parameters $\gamma = 1$ a.u., $v = 0.2$ a.u. and $\rho = 0.2, 0.5$ and 0.8 a.u. The branch points are labeled by the indices of the adiabatic states which are pairwise degenerate at these points. Due to the symmetry of the problem, branch points in other three quadrants of the complex τ -plane can be obtained as mirror images with respect to real and imaginary τ -axes. The most important for the collision dynamics are branch points which are closest to the real τ -axis. Thus the avoided crossing between the B -state and $n = 0$ state, visible in Figure 3, is the consequence of the proximity to the real τ -axis of the branch point $(B, 0)$ shown in Figure 4 in the $\rho = 0.5$ a.u. case. It can also be seen from Figure 4 that as the collisional impact parameter decreases the number of dynamic adiabatic eigenstates which are strongly coupled increases.

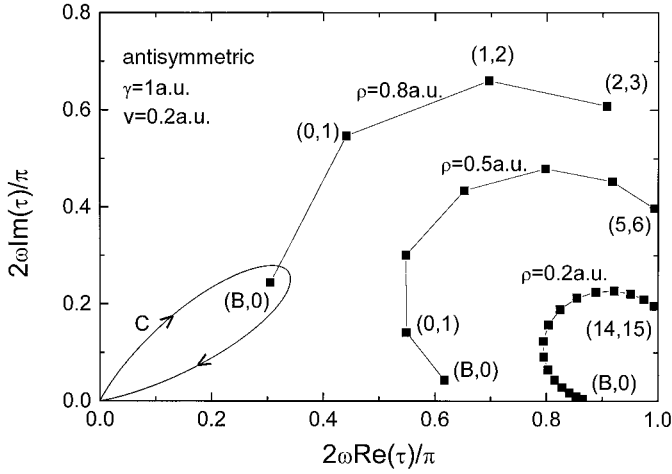


Fig. 4. Branch points of analytic continuations of antisymmetric dynamic adiabatic eigenvalue into complex τ -plane.

In what follows, we shall concentrate on the collisions with $\rho = 0.8$ a.u., where, as indicated from Figure 4, we can assume that only the coupling between the B and $n = 0$ states is important, whereas all other couplings can be neglected. Therefore, we are dealing with a two-state problem and the transition probability for populating the $n = 0$ antisymmetric state is [16]

$$|a_0^u(\tau_f)|^2 = 2e^{-2|B|}(1 - e^{-2|B|})\sin^2 A, \quad (3.16)$$

where A and B are real and imaginary parts of the integral

$$\int_C \varepsilon^u(\tau) d\tau = A + iB, \quad (3.17)$$

and contour C is shown in Figure 4. The probability (3.16) is one half the usual expression for the two-state problem [16], because of the initial condition (2.31). The integral in (3.17) can be calculated by applying integration by parts:

$$\int_C \varepsilon^u(\tau) d\tau = - \int_{C'} \tau(\varepsilon^u) d\varepsilon^u, \quad (3.18)$$

where C' is a contour (a semi-circle, for example) connecting the points $\varepsilon_B^u(\tau = 0)$ and $\varepsilon_0^u(\tau = 0)$ in the complex ε^u -plane. The function $\tau(\varepsilon^u)$ is explicitly given by (3.15) and (3.7). Numerical calculations give: $|a_0^u(\tau_f)|^2 = 0.064$.

We are now ready to calculate the momentum distribution, in the center-of-mass frame, of the detached electrons. According to (2.34), in our case we simply have

$$W(\mathbf{k}) = \frac{1}{v^3} |a_0^u(\tau_f)|^2 \left| \chi_0^u \left(\frac{\mathbf{k}}{v}, \tau_f \right) \right|^2. \quad (3.19)$$

Using the explicit expression (3.14) we first find the normalization constant

$$N_0 = \left(\frac{\omega}{\pi} \right)^{\frac{3}{4}} [2(1 - e^{-\frac{\omega}{v}})]^{-\frac{1}{2}}, \quad (3.20)$$

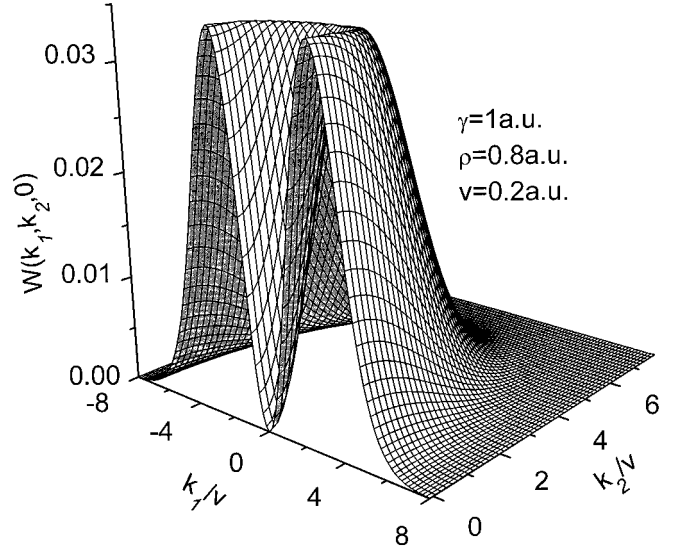


Fig. 5. Momentum distribution, in the center-of-mass frame, of the electrons ejected in the scattering plane ($k_3 = 0$).

and then from (3.19):

$$W(\mathbf{k}) = |a_0^u(\tau_f)|^2 \left(\frac{\rho}{\pi v} \right)^{\frac{3}{2}} \times \frac{\cosh(\rho k_1) - \cos(\rho k_2)}{2 \sinh\left(\frac{\rho v}{4}\right)} \exp\left(-\frac{\rho k^2}{v}\right). \quad (3.21)$$

As one can see from the above expression, in this case the form of the distribution does not depend on parameter γ (*i.e.* on electron-atom interaction) but has its origin in kinematics related to the selected trajectory of heavy particles. The electron-atom interaction determines the absolute value of the distribution through the probability of non-adiabatic transition (3.16).

Figure 5 shows the momentum distribution of the electrons ejected in the scattering plane ($k_3 = 0$). Only the $k_2 > 0$ region is shown in order to clearly make visible the minimum at the origin. The distribution is, of course, symmetric with respect to the k_1 -axis, $W(k_1, -k_2, 0) = W(k_1, k_2, 0)$. Almost cylindrical symmetry of the distribution is the consequence of the dumping effect of the exponent in (3.21). This dumping restricts the arguments of the cosh- and cos-function to the regions where these functions can be represented by the first two terms in their Taylor-series expansions:

$$W(\mathbf{k}) \approx |a_0^u(\tau_f)|^2 \left(\frac{\rho}{\pi v} \right)^{\frac{3}{2}} \frac{\rho^2(k_1^2 + k_2^2)}{4 \sinh\left(\frac{\rho v}{4}\right)} \times \exp\left(-\frac{\rho k^2}{v}\right). \quad (3.22)$$

From the last expression it follows that the maximum which appears in Figure 5 is located on the circle of radius $|\mathbf{k}| = (v/\rho)^{\frac{1}{2}}$.

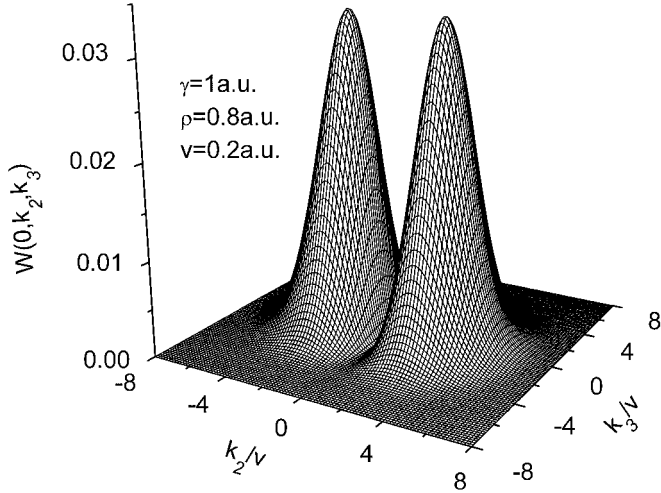


Fig. 6. Same as Figure 5, but in the plane perpendicular to the impact velocity ($k_1 = 0$).

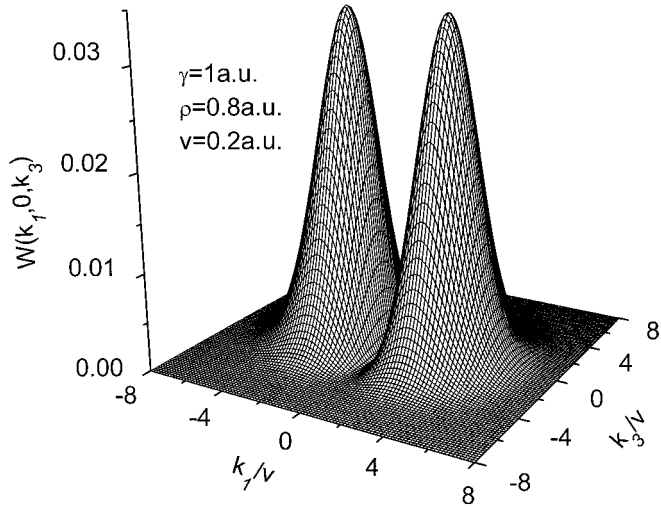


Fig. 7. Same as Figure 5, but in the plane perpendicular to the direction of the impact parameter ($k_2 = 0$).

Figures 6 and 7 show momentum distributions of the electrons ejected, respectively, in the plane perpendicular to the impact velocity ($k_1 = 0$) and in the plane perpendicular to the direction of the impact parameter ($k_2 = 0$). They appear almost indistinguishable due to the relation (3.22). The structures, such as the maxima in Figures 5, 6 and 7 and the minimum in Figure 5 are all consequences of the symmetry properties of the dynamic eigenstate which directly determine the momentum distribution via relation (3.19).

We have considered here the simplest situation when only the lowest C -type dynamic eigenstate is populated during the collision. As discussed above, in collisions with smaller impact parameters more states will be populated (although with successively decreasing probabilities) and, as can be seen from (2.34), one can expect complicated interference effects in the momentum distributions of the ejected electrons. We note also that the limit of head-on

collisions ($\rho \rightarrow 0, \omega \rightarrow 0$) needs the special treatment, and that exact expressions for the momentum distributions of the ejected electrons exist in this case [5, 11].

4 Concluding remarks

In order to fulfill the physical boundary conditions in the description of the slow atomic collisions, one is naturally led to the introduction of the new space and time-like variables and the notion of the dynamic adiabatic eigenstates. Basically, these eigenstates can be divided into two classes: the first one represents the states asymptotically localized in the vicinity of either of the centers of force and the second one represents the delocalized states. In physical space-time variables the first class corresponds to states which asymptotically represent the bound atomic states traveling with either of the force centers. The second class represents ever-spreading wavepackets and are related to the unbound motion of the electron.

The most important result of the present work is the expression (2.26) which relates the momentum distribution of the ejected electrons with a coherent sum of the delocalized dynamic adiabatic eigenstates (elementary wavepackets). The ionization or detachment process, in adiabatically slow collisions, proceeds via the population of these dynamic adiabatic eigenstates and the form of momentum distribution *exactly* coincides with the form of the total wavepacket in configuration space.

In the present application we have treated the model problem of electron detachment described by the zero-range potentials. Further developments will be directed towards the treatments of more realistic systems and interactions involving short-range as well as long-range (Coulomb) interactions.

Finally, we comment on the relationship between the present approximate theory and *ab initio* approach developed in references [12, 13]. The latter also employs the non-stationary scaling of length in order to ensure the correct boundary conditions. However, while in our method the resulting Schrödinger equation in $\{\mathbf{q}, \tau\}$ variables is solved approximately by using expansions in terms of dynamic adiabatic eigenstates, in references [12, 13] a method is developed for constructing the exact solutions. First, the Fourier transformation from τ to frequency domain is performed. The solution of the resulting equation is then expanded in terms of the Sturmian two-center functions which form a complete discrete basis. An increasing number of coupled equations for the expansion coefficients is solved numerically until the desired convergence is obtained. This method should give “exact” results (within the impact-parameter approximation) regardless of the magnitude of the relative collision velocity. The published applications [12, 13] are related to electron momentum distributions in head-on, proton-hydrogen collisions. It will certainly be interesting to compare in the future the predictions of both methods in the region of slow collisions.

This publication is based on work sponsored by the Macedonian - U.S. Joint Fund in cooperation with National Science Foundation under Project Number 100. T.P.G. acknowledges support from the Ministry of Science and Technology of the Republic of Serbia. E.A.S. is grateful for stimulating discussions with S. Ovchinnikov and J. Macek.

Appendix A

According to (2.25) and (2.24) the momentum distribution of the ejected electrons is given by

$$W(\mathbf{k}) = \left| \lim_{t \rightarrow +\infty} \sum_{\alpha_C} I(\mathbf{k}, t) e^{i\frac{1}{2}k^2 t} a_{\alpha_C}(\tau_f) e^{-i \int^{\tau_f} \varepsilon_{\alpha_C}(\tau) d\tau} \right|^2, \quad (\text{A.1})$$

where

$$I(\mathbf{k}, t) = (2\pi vt)^{-\frac{3}{2}} \int e^{-i\mathbf{k}\cdot\mathbf{r} + i\frac{z^2}{2t}} \chi_{\alpha_C} \left(\frac{\mathbf{r}}{vt}, \tau_f \right) d^3\mathbf{r} \quad (\text{A.2})$$

and we have used that for $t \rightarrow +\infty$, $R(t) \rightarrow vt$. Introducing the new integration variable $\mathbf{r} = t^{\frac{1}{2}}\mathbf{s}$, the above integral takes the form

$$I(\mathbf{k}, t) = (2\pi v)^{-\frac{3}{2}} \times \int e^{-it^{\frac{1}{2}}\mathbf{k}\cdot\mathbf{s} + i\frac{z^2}{2t}} \chi_{\alpha_C} \left(\frac{\mathbf{s}}{vt^{\frac{1}{2}}}, \tau_f \right) d^3\mathbf{s}. \quad (\text{A.3})$$

The above integral can be calculated by the saddle-point method. The position of the three-dimensional saddle-point is $\mathbf{s}_0 = t^{\frac{1}{2}}\mathbf{k}$. Note that the χ_{α_C} does not affect the position of the saddle-point even if it contains an exponential factor due to the $t^{-\frac{1}{2}}$ -dependence of its argument. We therefore arrive at the result

$$I(\mathbf{k}, t) = (iv)^{-\frac{3}{2}} e^{-i\frac{k^2 t}{2}} \chi_{\alpha_C} \left(\frac{\mathbf{k}}{v}, \tau_f \right). \quad (\text{A.4})$$

Substituting this back into (A.1) gives the expression (2.26).

Appendix B

We first note a general transformation property of the solutions of equation (2.15) with the translation of the origin of the reference frame along the q_1 -axis. Namely, the relationship between the solution $\chi(\mathbf{q}, \tau)$ with the origin at $(0, 0, 0)$ and the solution $\chi'(\mathbf{q}', \tau)$ with the origin at $(\alpha, 0, 0)$ is the following:

$$\chi(\mathbf{q}, \tau) = e^{-i\alpha\omega q_2} \chi'(\mathbf{q} - \alpha\hat{q}_1, \tau). \quad (\text{B.1})$$

This property can be checked by direct substitution of (B.1) in (2.15).

For the problem with two zero-range potentials the dynamic adiabatic eigenstates are solutions of the equation

$$\left(-\frac{1}{2}\nabla_{\mathbf{q}}^2 + \omega L_3 + \frac{1}{2}\omega^2 q^2 \right) \chi(\mathbf{q}, \tau) = \varepsilon(\tau)\chi(\mathbf{q}, \tau), \quad (\text{B.2})$$

which satisfy the boundary conditions:

$$\lim_{q_X \rightarrow 0} \chi(\mathbf{q}, \tau) \sim \text{const} \left[\frac{1}{q_X} - \gamma R(\tau) \pm \frac{i}{2}\omega \frac{q_2}{q_X} \right], \quad (\text{B.3})$$

$$X = T, P$$

with $\mathbf{q}_{T,P} = \mathbf{q} \pm \frac{1}{2}\hat{q}_1$. This conditions follow from (2.11) and (3.4).

Taking into account (B.1) we look for the symmetric and antisymmetric solutions of (B.2) and (B.3) in the form:

$$\chi^{g,u}(\mathbf{q}, \tau) = N \left[e^{\frac{i}{2}\omega q_2} \frac{U(q_T)}{q_T} \pm e^{-\frac{i}{2}\omega q_2} \frac{U(q_P)}{q_P} \right], \quad (\text{B.4})$$

where $U(q_X)$ is the solution of the equation

$$\left(-\frac{1}{2} \frac{d^2}{dq_X^2} + \frac{\omega^2}{2} q_X^2 - \varepsilon \right) U(q_X) = 0, \quad (\text{B.5})$$

satisfying the boundary conditions

$$\lim_{q_X \rightarrow 0} U(q_X) \sim c_0 + c_1 q_X, \quad \lim_{q_X \rightarrow \infty} U(q_X) = 0. \quad (\text{B.6})$$

The conditions (B.5) and (B.6) are uniquely satisfied by the parabolic-cylinder functions [15]:

$$U(q_X) = U \left(-\frac{\varepsilon}{\omega}, (2\omega)^{\frac{1}{2}} q_X \right). \quad (\text{B.7})$$

Substitution of (B.7) in (B.4) gives the expression (3.6) in the text, while the substitution of (B.4) in (B.3) reproduces the spectrum-determining equation (3.7).

We note that the spectrum of the unperturbed Hamiltonian in (B.2), that is without the boundary conditions (B.3), consists of series of discrete but infinitely-fold degenerate eigenvalues [9]:

$$\varepsilon_N = \omega \left(N + \frac{3}{2} \right), \quad N = 0, 1, 2, \dots \quad (\text{B.8})$$

With the introduction of the zero-range potentials, that is the boundary conditions (B.3), only one perturbed state per degenerate manifold with even N (of each g - and u -symmetry) emerges, as is seen from equation (3.13) in the text. The remaining states are not affected by the zero-range potentials and do not take part in the collision dynamics. The unperturbed manifolds with odd N are completely unaffected by the zero-range potentials because these states have odd parity $\Pi(q_3 \rightarrow -q_3) = (-1)^N$ [9] and are therefore exactly zero at the locations of the zero-range potentials.

References

1. D.R. Bates, R. McCarroll, Proc. Roy. Soc. Lond. A. **245**, 175 (1958).
2. S.B. Schneiderman, A. Russek, Phys. Rev. A **181**, 311 (1969).
3. J.B. Delos, Rev. Mod. Phys. **53**, 287 (1981).
4. L.F. Errea, L. Mandez, A. Riera, J. Phys. B: At. Mol. Opt. Phys. **15**, 101 (1982).
5. E.A. Solov'ev, Teor. Mat. Fiz. **28**, 240 (1976) [Theor. Mat. Phys. (USSR) **28**, 575 (1976)].
6. E.A. Solov'ev, S.I. Vinitsky, J. Phys. B: At. Mol. Opt. Phys. **18**, L557 (1985).
7. E.A. Solov'ev, Usp. Fiz. Nauk. **157**, 437 (1989) [Sov. Phys. Usp. **32**, 228 (1989)].
8. T.P. Grozdanov, E.A. Solov'ev, Phys. Rev. A **42**, 2703 (1990).
9. T.P. Grozdanov, E.A. Solov'ev, Phys. Rev. A **44**, 5605 (1991).
10. E.A. Solov'ev, Zh. Eksp. Teor. Fiz. **70**, 872 (1976) [Sov. Phys. JETP **43**, 435 (1976)].
11. M. Raković, E.A. Solov'ev, Phys. Rev. A **41**, 3635 (1990).
12. S. Ovchinnikov, J. Macek, Phys. Rev. Lett. **75**, 2474 (1995).
13. S. Ovchinnikov, J. Macek, D.B. Khrebtukov, Phys. Rev. A **56**, 2872 (1997).
14. Yu. Demkov, V.N. Ostrovskii, *Zero-Range Potentials and Their Applications in Atomic Physics* (Plenum, New York, 1988).
15. M. Abramowitz, I.A. Stegun, *Handbook of Mathematical Functions* (Dover, New York, 1965).
16. R.K. Janev, J. Pop-Jordanov, E.A. Solov'ev, J.Phys. B: At. Mol. Opt. Phys. **30**, L353 (1997).